

# 000 PLP-NER: Point-Line-Plane Fusion for Named Entity 001 Recognition with BERT 002 003 004

005 Anonymous authors  
006 Paper under double-blind review  
007  
008  
009

## 010 Abstract 011

012 Current state-of-the-art Named Entity Recognition systems commonly  
013 leverage an architecture that integrates BERT with Conditional Random  
014 Fields. Nevertheless, BERT is inherently constrained in capturing compre-  
015 hensive global contextual semantics due to its Masked Language Modeling  
016 pre-training objective. To address this limitation, A novel “point–line–  
017 plane” contextual fusion framework is proposed. Within this paradigm,  
018 the [CLS] token functions as a “plane” that provides a compressed global  
019 representation, while the attention weights between the [CLS] token and  
020 individual tokens form a “line”, which captures semantic topological re-  
021 lationships. These multi-grained features are subsequently incorporated  
022 into token representations via a Graph Neural Network, considerably en-  
023 riching their contextual expressiveness. Furthermore, we introduce a Dy-  
024 namic Linear-Chain CRF that adaptively models label transitions using  
025 attention-mechanized probability estimates, thereby overcoming the inflex-  
026 ibility of conventional CRFs. Extensive experiments on multiple benchmark  
027 datasets demonstrate that our approach consistently and significantly sur-  
028 passes competitive baselines, achieving a notable 3.91 point gain in F1-  
029 score.  
030

## 031 1 INTRODUCTION 032

033 Named Entity Recognition (NER) is a core task in natural language processing (NLP)  
034 that identifies and classifies named entities such as people, organizations, and locations in  
035 unstructured text (Nadeau & Sekine (2007)). As a fundamental component of the NLP  
036 pipeline, NER underpins a wide range of downstream applications, including information  
037 extraction, question answering, and knowledge graph construction. The task involves two  
038 key steps: entity span detection, which identifies the boundaries of an entity, and entity  
039 type classification, which assigns its semantic category (Luo et al. (2019)).

040 Early NER research relied on rule-based and statistical learning methods (Grishman &  
041 Sundheim (1996), Nadeau & Sekine (2007)). While effective in their time, these approaches  
042 were limited by their reliance on handcrafted features and shallow semantic understanding  
043 (Augenstein et al. (2017), Bengio et al. (2003)). The field was revolutionized by the ad-  
044 vent of Transformer-based pre-trained language models (PLMs), such as BERT (Vaswani  
045 et al. (2017), Devlin et al. (2019)) These models leverage self-attention mechanisms to gen-  
046 erate rich, contextualized representations, significantly advancing the state of the art in  
047 NER. Architectures that combine PLMs with a Conditional Random Field (CRF) layer,  
048 like BERT-CRF, have become standard baselines, marrying the semantic power of Trans-  
049 formers with the global sequence decoding capabilities of CRFs (Devlin et al. (2019), Huang  
et al. (2015)).

050 Despite their success, current PLM-based models for NER face several notable challenges.  
051 The pre-training objective, typically Masked Language Modeling (MLM), can lead to incom-  
052 plete contextual semantics for the fine-grained NER task(Meng et al. (2024)). Furthermore,  
053 the pretraining–finetuning divergence introduces a representation shift that can degrade  
model performance and generalization (Villena et al. (2024), Cui et al. (2020)). Finally,

while CRFs enhance decoding, their static transition structure is rigid and fails to adapt to the specific semantic correlations present in different input sentences (Wang & Ji (2022)).

To address these limitations, we propose a novel Point–Line–Plane Fusion Framework for NER (PLP-NER). Our framework is designed to enrich semantic representation, improve structural adaptability, and enhance model generalization. Our key contributions are as follows:

- Multi-level Contextual Fusion: 1. We introduce a point–line–plane mechanism that effectively integrates token-level, pairwise, and global representations, enriched by graph neural networks, to capture more comprehensive semantic relationships.
- Dynamic Sequence Decoding: We design a dynamic linear-chain CRF that computes input-specific transition probabilities, enabling more flexible and context-sensitive label prediction.
- Masking-based Embedding Strategy: 3. We employ a novel masking mechanism during training to mitigate the pretraining–finetuning divergence, thereby improving the model’s robustness and generalization.

Extensive experiments on multiple benchmark datasets demonstrate that our framework consistently outperforms strong baselines, achieving an average F1-score improvement of 3.91 points. These results confirm the effectiveness of our approach in pushing the boundaries of NER performance.

Experimental results on multiple standard NER benchmarks demonstrate that the proposed contextual information fusion mechanism consistently achieves significant performance improvements over current SOTA methods. Specifically, our approach yields F1-score gains of 3.91 percentage points across several datasets, comprehensively validating its effectiveness in enhancing model performance and robustness, as well as advancing capabilities in semantic representation, structural adaptability, and generalization.

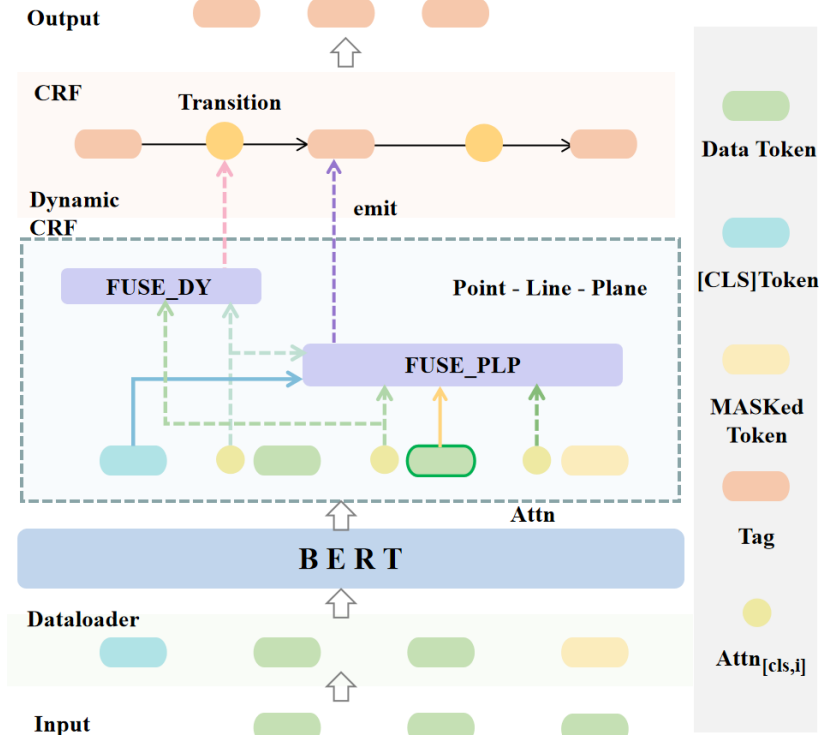


Figure 1: Point-Line-Plane Fusion Frame Diagram

108 

## 2 RELATED WORK

109  
110 The field of Named Entity Recognition (NER) has undergone a significant evolution, pro-  
111 gressing from early rule-based systems to sophisticated deep learning and pre-trained models.  
112113 

### 2.1 Main Approaches In NER.

114 

#### 2.1.1 Rule-based and Statistical Models.

115  
116 Early NER systems were largely based on handcrafted rules, dictionaries, and lexicons (Gr-  
117 ishman & Sundheim (1996)). While precise for specific domains, these methods were labor-  
118 intensive to develop, brittle, and lacked the generalization capacity needed for diverse text.  
119 The field subsequently moved toward statistical models, which framed NER as a sequence  
120 labeling task. Probabilistic models like Hidden Markov Models (HMMs) (Rabiner (1989)),  
121 Maximum Entropy Models (MEMs) (Berger et al. (1996)), and, most notably, Conditional  
122 Random Fields (CRFs) (Lafferty et al. (2001)) became standard. CRFs were particularly ef-  
123 fective due to their ability to model global dependencies and avoid the strong independence  
124 assumptions of HMMs. However, these models were still limited by their reliance on shallow,  
125 manually engineered features and struggled to capture long-range semantic context.  
126127 

#### 2.1.2 Neural Representation Learning

128  
129 The advent of deep learning introduced a paradigm shift by enabling models to learn features  
130 automatically. Recurrent Neural Networks (RNNs), particularly Long Short-Term Memory  
131 (LSTM)(Hochreiter & Schmidhuber (1997)) networks, proved adept at capturing sequential  
132 dependencies. The BiLSTM-CRF architecture (Huang et al. (2015)) became a popular and  
133 powerful model, combining the sequential feature learning of a bidirectional LSTM with  
134 the global sequence decoding of a CRF. This combination improved consistency in label  
135 predictions and handled out-of-vocabulary words more robustly. Other neural architectures,  
136 such as Convolutional Neural Networks (CNNs) (Ma & Hovy (2016)), were also used to  
137 extract local features from character and word embeddings. Despite these improvements,  
138 these models still faced limitations in capturing global, document-level context due to the  
139 nature of their sequential processing.  
140141 

#### 2.1.3 Pre-trained Language Models (PLMs)

142  
143 The most significant recent breakthrough in NER has been the adoption of large-scale pre-  
144 trained language models (PLMs) based on the Transformer architecture (Vaswani et al.  
145 (2017)). Models like BERT (Devlin et al. (2019)), RoBERTa (Liu et al. (2019)), and Span-  
146 BERT (Joshi et al. (2020)) are pre-trained on massive text corpora to learn deep, context-  
147 ualized representations, which can then be fine-tuned for downstream tasks like NER. The  
148 standard BERT-CRF architecture, which uses BERT as an encoder to produce rich con-  
149 textual embeddings and a CRF layer for structured prediction, has become the dominant  
150 discriminative approach in the field. These models have set new state-of-the-art results  
151 across a wide range of NER benchmarks.  
152153 

## 2.2 Recent Trends and Limitations

154  
155 While PLMs have propelled NER to new heights, several active research areas aim to address  
156 their remaining limitations. One direction is exploring generative approaches, which frame  
157 NER as a text-to-text task using models like T5 (Raffel et al. (2019)) or GPT (Brown et al.  
158 (2020)) (Yan et al. (2021)). These methods can handle complex nested and discontinuous  
159 entities but often come with high computational costs and remain less widely adopted than  
160 discriminative models. Another trend is retrieval-augmented NER, which uses external  
161 knowledge bases to enrich entity representations and handle low-resource or unseen entities  
(Lewis et al. (2020)).162  
163 Despite their effectiveness, current PLM-based models still face challenges related to se-  
164 mantic fusion and domain adaptability. Fine-tuning a pre-trained model on a new domain  
165 can lead to a pretraining–finetuning divergence, where the representations shift, hurting  
166

162 performance (Liu et al. (2021)). Furthermore, the static nature of standard CRF transition  
 163 probabilities limits their ability to capture fine-grained, input-specific semantic correlations.  
 164 Our work builds upon the powerful BERT-CRF framework and introduces novel mechanisms  
 165 to address these specific challenges through multi-level contextual fusion, dynamic decoding,  
 166 and a masking-based training strategy.  
 167

### 168 3 METHODOLOGY

#### 170 3.1 Preliminaries

172 NER is a sequence labeling task. Given an input sequence  $X = (x_1, x_2, \dots, x_n)$ , the objective  
 173 is to predict the corresponding label sequence  $Y = (y_1, y_2, \dots, y_n)$ . Our approach is built  
 174 upon the well-established BERT+CRF framework, which models the conditional probability  
 175 of the label sequence  $P(Y | X)$  by maximizing its likelihood. The training process involves  
 176 minimizing the negative log-likelihood loss:

$$177 \mathcal{L}(\theta, \varphi, T) = -\log P(Y^* | X, \theta, \varphi, T) = - \left[ \text{score}(Y^*, X; \theta, \varphi, T) - \log \left( \sum_{Y \in \mathcal{Y}(X)} \exp(\text{score}(Y, X; \theta, \varphi, T)) \right) \right] \quad (1)$$

181 The sequence score is defined as the sum of emission and transition scores:

$$183 \text{score}(Y, X; \theta, \varphi, T) = \sum_{i=1}^n E_\varphi(B_\theta(x_i | X)) + \sum_{i=1}^{n-1} T_{y_i, y_{i+1}} \quad (2)$$

186 Here,  $B_\theta(\cdot)$  denotes the token representation from BERT,  $E_\varphi(\cdot)$  is the emission score function,  
 187 and  $T_{y_i, y_{i+1}}$  is the transition score from a static, learnable matrix  $T$ . This framework  
 188 serves as our foundational baseline due to its effectiveness in balancing semantic representation  
 189 and structured decoding.

#### 191 3.2 Point–Line–Plane Contextual Fusion

193 While BERT+CRF is powerful, it suffers from insufficient contextual fusion. The representations from BERT, trained with objectives like MLM and NSP, often lack a comprehensive  
 194 understanding of global semantic structure. To address this, we propose the Point–Line–  
 195 Plane (PLP) Contextual Fusion mechanism, which draws an analogy from geometry to  
 196 enhance structured semantic modeling.

- 198 • Semantic Points: We treat each token embedding,  $B_\theta(x_i | X)$ , as a semantic point,  
 199 representing the local contextual semantics of an individual token.
- 200 • Semantic Plane: The [CLS] token,  $B_\theta(\text{CLS} | X)$ , serves as a semantic plane, pro-  
 201 viding a compressed representation of the global context.
- 202 • Semantic Lines: The attention weights between the [CLS] token and each word to-  
 203 ken,  $a_\theta(x_i | X) = \text{Attn}_\theta(\text{CLS} \rightarrow x_i | X)$ , are conceptualized as semantic lines. They  
 204 explicitly capture the topological relationship between local and global contexts.

206 This framework can be viewed as a simplified Graph Neural Network (GNN) where the  
 207 [CLS] node is a central hub for all other token nodes. Our approach enhances the emission  
 208 score function  $E_\varphi$  of the CRF to incorporate these multi-level representations, resulting in  
 209 a new functional form:

$$211 E_i = f(B_\theta(x_i | X), B_\theta(\text{CLS} | X), a_\theta(x_i | X)) \quad (3)$$

212 This function enriches each token’s representation with global and structural information  
 213 before it is passed to the CRF. We implement this fusion using a two-stage Multi-Layer  
 214 Perceptron (MLP):  
 215

$$f(\cdot) = \text{MLP}(\text{MLP}(B_\theta(\text{CLS} | X) \oplus a_\theta(x_i | X)) \oplus B_\theta(x_i | X)) \quad (4)$$

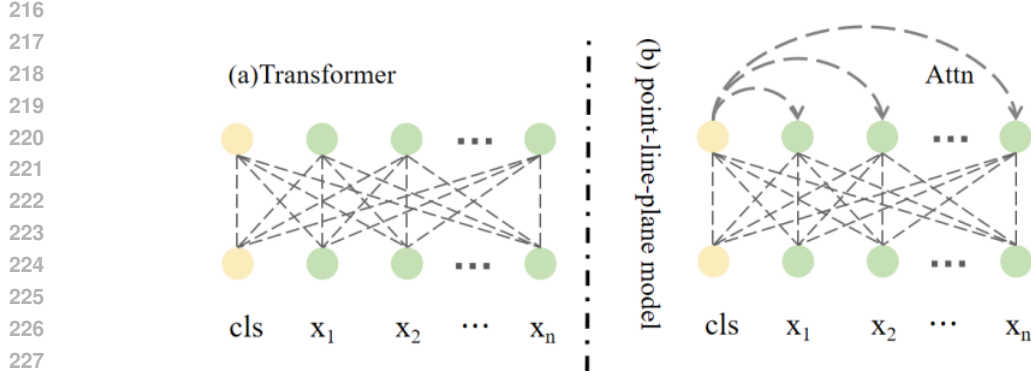


Figure 2: Geometric schematic diagram of Point-Line-Plane integration modeling based on transformer architecture.

where  $\oplus$  denotes vector concatenation. This two-stage process ensures a deeper integration of global and structural information into the token-level representations.

To further enhance the robustness of boundary detection, we introduce Neighborhood Enhancement based on our observation that attention weights between adjacent tokens and the [CLS] token provide strong cues for entity boundaries and label consistency. We modify the fusion function to incorporate these neighborhood features:

$$f(\cdot) = \text{MLP}(\text{MLP}(B_\theta(\text{CLS}|X) \oplus a_\theta(x_{i-1} : x_{i+1}|X)) \oplus B_\theta(x_i|X)) \quad (5)$$

This new function explicitly leverages local interaction patterns to inform the model, enhancing its ability to handle complex entity boundaries.

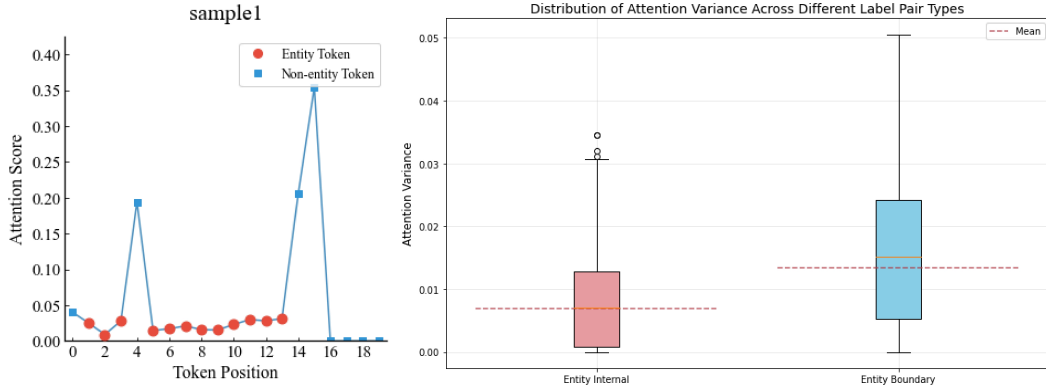


Figure 3: Statistical Results of Differences in Attention Scores Between Entity Boundary and Internal Tokens Towards the CLS Token and Sample Line Chart Display.

### 3.3 Dynamic Linear-Chain CRF

Standard CRFs use a static transition matrix  $T$  that encodes global, corpus-level statistics. This rigidity makes it difficult to adapt to a specific sentence's context, leading to suboptimal predictions for complex or ambiguous transitions. To overcome this, we propose a Dynamic Linear-Chain CRF that modifies transition scores based on local, input-specific features.

Our attention visualization analysis reveals that attention patterns show high consistency within entities and sharp changes at boundaries (see Figure 3). Motivated by this, we use the attention scores of adjacent tokens to the [CLS] token as features for dynamic transition adjustments. We define a mapping function  $g_\beta : \mathbb{R}^d \rightarrow \mathbb{R}^3$  to produce a 3-dimensional vector  $v_i = (g_\beta^{\text{in}}(s_i), g_\beta^{\text{bd}}(s_i), g_\beta^{\text{out}}(s_i))$ , where  $s_i = [\text{Attn}(x_i, \text{cls}|X), \text{Attn}(x_{i+1}, \text{cls}|X)]$ . These

270 components are designed to correct transitions within entities ( $g^{\text{in}}$ ), across entity boundaries  
 271 ( $g^{\text{bd}}$ ), and between non-entities ( $g^{\text{out}}$ ).

273 To apply these corrections, we define a label transition index function  $\kappa : Y \times Y \rightarrow \{0, 1, 2\}$ ,  
 274 which assigns an index to each type of transition (e.g., 'B-PER' to 'I-PER' is an 'in-entity'  
 275 transition). The dynamic transition score is then defined as:

$$276 \quad D_\beta(y_i, y_{i+1}) = T_{y_i y_{i+1}} + \sum_{k=0}^2 v_{i,k} \cdot \mathbb{I}[\kappa(y_i, y_{i+1}) = k] \quad (6)$$

278 This function modifies the base transition score  $T_{y_i y_{i+1}}$  with a context-dependent correction  
 279  $v_{i,k}$ . We apply symmetric clipping to keep these dynamic adjustments within a small, stable  
 280 range, preventing the model from becoming unstable while still allowing for fine-grained  
 281 adjustments.

282 The overall sequence score becomes:

$$284 \quad \text{score}(Y, X) = \sum_{i=1}^n e_{i,y_i} + \sum_{i=1}^{n-1} D_\beta(y_i, y_{i+1}) \quad (7)$$

286 This hierarchical approach of "feature encoding - index mapping - dynamic correction"  
 287 ensures that our model can adapt its transition probabilities to the specific context of each  
 288 sequence, significantly improving its generalization capacity.

### 290 3.4 Training Objective

292 To mitigate the pretraining–finetuning mismatch and improve the robustness of our model,  
 293 we incorporate a second objective. Similar to BERT’s original training, we add an auxiliary  
 294 Masked Language Modeling (MLM) loss. During training, we randomly mask 15% of the  
 295 input tokens and train the model to reconstruct them. This auxiliary task forces the model  
 296 to maintain its pre-trained semantic understanding, reducing the representation shift that  
 297 often occurs during fine-tuning. Our final optimization objective is a combination of the  
 298 primary NER loss and the auxiliary MLM loss:

$$299 \quad \mathcal{L}(\theta, \varphi, \beta, \mathbf{T}) = \mathcal{L}_{\text{ner}}(\theta, \varphi, \beta, \mathbf{T}) + \mathcal{L}_{\text{mlm}}(\theta) \quad (8)$$

300 This joint training strategy leverages the best of both worlds, ensuring that the model  
 301 remains sensitive to fine-grained token-level semantics while optimizing for the primary  
 302 NER task.

## 303 4 EXPERIMENT

### 306 4.1 Datasets

307 To rigorously evaluate the effectiveness and generalization of the proposed method, we con-  
 308 duct experiments on four representative Chinese and English NER benchmarks—specifically  
 309 including CoNLL2003 (English general-domain), WNUT17 (English low-resource), MSRA  
 310 (Chinese general-domain), and CLUENER (Chinese domain-specific)—which span general-  
 311 domain, low-resource, and domain-specific settings.

### 313 4.2 Implementation Details

315 We adopt the F1 score as the evaluation metric to assess model performance, defined as  
 316 follows:

$$317 \quad \text{F1} = 2 \times \frac{\text{Precision} \times \text{Recall}}{\text{Precision} + \text{Recall}}, \text{Precision} = \frac{TP}{TP + FP}, \text{Recall} = \frac{TP}{TP + FN}$$

319 where  $TP$ ,  $FP$ , and  $FN$  denote true positives, false positives, and false negatives, respec-  
 320 tively.

321 All experiments are implemented based on the BERT+CRF framework. We utilize the  
 322 Hugging Face Transformers library to load pretrained models and tokenizers. Training  
 323 is conducted on two NVIDIA GPUs, with the core hyperparameters and configurations  
 summarized as follows:

324

325

Table 1: Statistics of Benchmark Datasets for NER Evaluation

326

327

Dataset	Language	Train/Dev/Test	Entity Categories
CoNLL-2003	English	14,987 / 3,466 / 3,684	Person,Organization,Location, MISC
WNUT2017	English	1,000 / 128 / 1,283	Person,Location,Organization, Product,Event,Corporation
MSRA	Chinese	46,364 / - / 4,365	Person,Location,Organization
CLUENER	Chinese	10,748 / 1,343 / 1,345	Address,Book,Company,Game, Government,Movie,Name, Organization,Position,Scene

335

336

337

Table 2: Hyperparameter Settings

338

339

Parameter	Value
Maximum sequence length	512
Batch size per GPU	12
Optimizer	AdamW
Learning rate for BERT backbone	3e-5
Learning rate for dynamic CRF layer	1e-3
Learning rate for masking task	1e-3
Maximum training epochs	10

340

341

342

343

344

345

346

347

348

349

### 4.3 Results And Analyse

350

351

352

Table 3: Experimental Results on CoNLL-2003, WNUT-2017, MSRA, and CLUENER

353

Dataset/F1	CoNLL2003	WNUT2017	MSRA	CLUENER
<b>SOTA</b>				
BERT+MRC+DSC(Li et al. (2020))	93.95	-	96.72	77.56
ACE+document-context(Wang et al. (2020))	94.60	-	-	-
W2NER(Li et al. (2021))	93.07	-	96.10	-
<b>Baseline</b>				
BERT+CRF	93.95	60.14	94.41	80.76
<b>Ours</b>				
PLP-NER	94.51	60.53	95.85	81.57
+MASK	94.60	61.09	96.15	82.27
+NE	94.93	61.39	96.93	84.12
+DY	95.07	60.77	96.89	84.67

364

We conducted a systematic comparison of our innovative model with baseline models, representative historical methods, and the current SOTA NER models. As shown in Table 3, we employ the macro-average F1 score on the test set as the quantitative evaluation metric for model performance. The experimental results demonstrate that the PLPA model consistently exhibits superior performance across all benchmark datasets.

365

366

367

368

369

370

371

372

373

374

375

376

377

It is noteworthy that the introduction of the Dynamic Linear-Chain CRF resulted in slight fluctuations in performance on the WNUT-17 dataset. This could be attributed to the relatively small size of the dataset, where the complex dynamic transition matrix increases the risk of overfitting. Nevertheless, our model still significantly outperforms the baseline methods under this setup. Particularly, on the fine-grained entity recognition benchmark CLUENER, the PLPA model achieves a substantial 3.91 percentage points improvement. This breakthrough can be attributed to two key factors: firstly, the current SOTA methods for this dataset still leave considerable room for improvement in fine-grained entity recognition; secondly, the attention-based scoring mechanism we propose effectively models the

378 boundary features of multi-class fine-grained entities, a task that existing methods struggle  
 379 with due to their limited ability to perceive such complex boundary patterns.  
 380

381 Overall, a comprehensive analysis of the experimental results reveals that our proposed  
 382 model demonstrates significant advantages in terms of generalization, robustness, and recog-  
 383 nition accuracy. In particular, in the context of fine-grained entity recognition, the model's  
 384 robust capability to model complex boundary patterns provides new insights and power-  
 385 ful tools for advancing NER technology, showcasing its considerable research value and  
 386 application potential.  
 387

#### 388 4.4 Ablation

389 As shown in Table 3, the stepwise ablation experiments verify the incremental contribution  
 390 of each component:  
 391

- 392 • PLP-NER (base). Delivers consistent gains over BERT+CRF across four  
 393 benchmarks (CoNLL-2003, WNUT-2017, MSRA, CLUENER), lifting F1 by  
 394  $+0.56/+0.39/+1.44/+0.81$ , indicating that point–line–plane fusion improves token-  
 395 , span-, and structure-level interactions.
- 396 • +MASK. Provides further steady improvements of  $+0.09/+0.56/+0.30/+0.70$  over  
 397 PLP-NER, mitigating the train–test mismatch and enhancing generalization.
- 398 • +NE. Yields the largest incremental gains, especially on MSRA (+0.78) and  
 399 CLUENER (+1.85), highlighting the importance of local context for boundary de-  
 400 tection.
- 401 • +DY. Achieves the best overall F1 on CoNLL-2003 (95.07), MSRA (96.89), and  
 402 CLUENER (84.67); on WNUT-2017, +DY is slightly lower than +NE (60.77 vs.  
 403 61.39) yet remains  $+0.63$  above BERT+CRF.

404 Overall, the ablation trend suggests that (i) multi-granularity fusion (PLP-NER) establishes  
 405 a strong foundation, (ii) regularized training (+MASK) yields stable gains, (iii) local context  
 406 (+NE) is crucial for hard boundaries, and (iv) label-dependent dynamics (+DY) provide  
 407 the final push to state-of-the-art performance on three datasets.  
 408

## 409 5 CONCLUSION

410 In this paper, we present an enhanced BERT-CRF framework that integrates semantic  
 411 fusion, dynamic structural modeling, and training strategies, achieving significant gains in  
 412 accuracy and robustness across multiple NER benchmarks.  
 413

## 414 Acknowledgments

415 We used a large language model-based assistant during the final editing stage for language  
 416 polishing (grammar, clarity, and style). The tool did not contribute to the research design,  
 417 experiments, data analysis, or claims; the authors remain solely responsible for all content  
 418 and any errors. We complied with ICLR's policy on responsible use of generative tools and  
 419 manually verified outputs to avoid inclusion of unauthorized or sensitive material.  
 420

## 421 References

422 Isabelle Augenstein, Leon Derczynski, and Kalina Bontcheva. Generalisation in named  
 423 entity recognition: A quantitative analysis. *Computer Speech & Language*, 44:61–83,  
 424 2017.

425 Yoshua Bengio, Réjean Ducharme, Pascal Vincent, and Christian Jauvin. A neural proba-  
 426 bilistic language model. *Journal of Machine Learning Research*, 3:1137–1155, 2003.

427 Adam L. Berger, Stephen A. Della Pietra, and Vincent J. Della Pietra. A maximum entropy  
 428 approach to natural language processing. *Computational Linguistics*, 22(1):39–71, 1996.

432 Tom B. Brown, Benjamin Mann, Nick Ryder, Melanie Subbiah, and Dario Amodei. Lan-  
 433 guage models are few-shot learners. 2020.

434

435 Yiming Cui, Wanxiang Che, Ting Liu, Bing Qin, Ziqing Yang, Shijin Wang, and Guoping  
 436 Hu. Macbert: Mlm as correction bert for chinese nlp. arXiv preprint arXiv:2009.00972,  
 437 2020.

438

439 Jacob Devlin, Ming-Wei Chang, Kenton Lee, and Kristina Toutanova. Bert: Pre-  
 440 training of deep bidirectional transformers for language understanding. arXiv preprint  
 441 arXiv:1810.04805, 2019.

442

443 Ralph Grishman and Beth Sundheim. Message understanding conference 6: A brief his-  
 444 tory. In Proceedings of the 16th Conference on Computational Linguistics, Volume 1.  
 445 Association for Computational Linguistics, 1996.

446

447 Sepp Hochreiter and Jürgen Schmidhuber. Long short-term memory. *Neural Computation*,  
 9(8):1735–1780, 1997.

448

449 Zhiheng Huang, Wei Xu, and Kai Yu. Bidirectional lstm-crf models for sequence tagging.  
 450 In Proceedings of the Computer Science Conference, 2015.

451

452 Mandar Joshi, Danqi Chen, Yinhan Liu, Daniel S. Weld, Luke Zettlemoyer, and Omer Levy.  
 453 Spanbert: Improving pre-training by representing and predicting spans. *Transactions of  
 454 the Association for Computational Linguistics*, 8:64–77, 2020.

455

456 John Lafferty, Andrew McCallum, and Fernando Pereira. Conditional random fields: Prob-  
 457 abilistic models for segmenting and labeling sequence data. In Proceedings of the Eight-  
 458eenth International Conference on Machine Learning, pp. 282–289, 2001.

459

460 Patrick Lewis, Ethan Perez, Aleksandra Piktus, Fabio Petroni, Vladimir Karpukhin, Naman  
 461 Goyal, Heinrich Küttler, Mike Lewis, Wen tau Yih, Tim Rocktäschel, Sebastian Riedel,  
 462 and Douwe Kiela. Retrieval-augmented generation for knowledge-intensive nlp tasks. In  
 463 Proceedings of Advances in Neural Information Processing Systems, 2020.

464

465 Jingye Li, Hao Fei, Jiang Liu, Shengqiong Wu, Meishan Zhang, Chong Teng, Donghong Ji,  
 466 and Fei Li. Unified named entity recognition as word-word relation classification. arXiv  
 467 e-prints, 2021.

468

469 Xiaoya Li, Xiaofei Sun, Yuxian Meng, Junjun Liang, and Jiwei Li. Dice loss for data-  
 470 imbalanced nlp tasks. In Proceedings of the 58th Annual Meeting of the Association for  
 471 Computational Linguistics, 2020.

472

473 Tianyu Liu, Kexin Wang, Aadesh Jha, and Mrinmaya Sachan. Revisiting pre-training  
 474 for natural language processing. In Proceedings of the 2021 Conference of the North  
 475 American Chapter of the Association for Computational Linguistics: Human Language  
 476 Technologies, pp. 1–10, 2021.

477

478 Yinhan Liu, Myle Ott, Naman Goyal, Jingfei Du, Mandar Joshi, Danqi Chen, Omer Levy,  
 479 Mike Lewis, Luke Zettlemoyer, and Veselin Stoyanov. Roberta: A robustly optimized  
 480 bert pretraining approach. arXiv preprint arXiv:1907.11692, 2019.

481

482 Yong Luo, Hongyu Zhang, Dinghan Shen, and et al. A boundary-aware neural model for  
 483 nested named entity recognition. In Proceedings of the 2019 Conference on Empirical  
 484 Methods in Natural Language Processing and the 9th International Joint Conference  
 485 on Natural Language Processing (EMNLP-IJCNLP), pp. 5799–5808, Hong Kong, China,  
 2019. Association for Computational Linguistics.

486

487 Xuezhe Ma and Eduard Hovy. End-to-end sequence labeling via bi-directional lstm-cnns-crf.  
 488 In Proceedings of the Annual Meeting of the Association for Computational Linguistics,  
 489 pp. 1064–1074, 2016.

486 Yu Meng, Jitin Krishnan, Sinong Wang, Qifan Wang, Yuning Mao, Han Fang, Mar-  
 487 jan Ghazvininejad, Jiawei Han, and Luke Zettlemoyer. Representation deficiency in  
 488 masked language modeling. In B. Kim, Y. Yue, S. Chaudhuri, K. Fragkiadaki, M. Khan,  
 489 and Y. Sun (eds.), International Conference on Representation Learning, volume 2024,  
 490 pp. 44071–44091, 2024. URL [https://proceedings iclr cc/paper\\_files/paper/2024/file/bfde7fb279709eff53faa074b45840d8-Paper-Conference.pdf](https://proceedings iclr cc/paper_files/paper/2024/file/bfde7fb279709eff53faa074b45840d8-Paper-Conference.pdf).

492 David Nadeau and Satoshi Sekine. A survey of named entity recognition and classification.  
 493 Lingvisticae Investigationes, 30(1):3–26, 2007.

494

495 Lawrence R. Rabiner. A tutorial on hidden markov models and selected applications in  
 496 speech recognition. Proceedings of the IEEE, 77(2):257–286, 1989.

497

498 Colin Raffel, Noam Shazeer, Adam Roberts, Katherine Lee, Sharan Narang, Michael  
 499 Matena, Yanqi Zhou, Wei Li, and Peter J. Liu. Exploring the limits of transfer learning  
 500 with a unified text-to-text transformer. 2019.

501

502 Ashish Vaswani, Noam Shazeer, Niki Parmar, Jakob Uszkoreit, Llion Jones, Aidan N.  
 503 Gomez, Çukasz Kaiser, and Illia Polosukhin. Attention is all you need. In Proceedings of  
 504 Advances in Neural Information Processing Systems, pp. 5998–6008, 2017.

505

506 Fabián Villena, Luis Miranda, and Claudio Aracena. llmner: (zero|few)-shot named  
 507 entity recognition, exploiting the power of large language models. arXiv preprint  
 508 arXiv:2406.04528, 2024. URL <https://arxiv.org/abs/2406.04528>. arXiv:2406.04528  
 509 [cs.CL].

510

511 Xinyu Wang, Yong Jiang, Nguyen Bach, Tao Wang, and Kewei Tu. Automated concatenation  
 512 of embeddings for structured prediction. 2020.

513

514 Yifan Wang and Qi Ji. A dynamic conditional random field model for object segmentation  
 515 in image sequences. In Proceedings of the European Conference on Computer Vision,  
 516 2022.

517

518

519

520

521

522

523

524

525

526

527

528

529

530

531

532

533

534

535

536

537

538

539